Chapter 8
Cusp-Field Single-Pole-Type (CF-SPT) Head for Perpendicular Recording

Kiyoshi Yamakawa

8.1 Introduction of CF-SPT Head

Maintaining the thermal stability of small magnetic grains is important for perpendicular magnetic recording; for achieving higher recording densities, it is inperative to continue to increase the strength and sharpness of the magnetic recording field of single-pole-type (SPT) heads because the anisotropy energy of the recording media becomes large, thereby threatening the thermal stability. Development of soft magnetic pole material with a high saturation magnetic flux density, B_s, is the first requirement. Furthermore, improvement of the head structure is important because little room is left for the B_s increasing to its practical limit of 2.45 T.

The first single-pole head was developed as an auxiliary-pole-driven-type head [1]. This head underscored the importance of the head-energizing method for realizing a strong and sharp recording field in which the coil created the strongest field at the top in the main pole located at the air-bearing surface (ABS). This concept was inherited by the thin film SPT head [2] depicted in Fig. 8.1a. In the head, the coil of the helical structure is wound closely around the main pole throat to excite the pole tip directly with the strongest coil field. As depicted in Fig. 8.1b, field calculations reveal that the highest head field was obtained when the coil recession height, h, from the ABS was zero.

The cusp-field single-pole type (CF-SPT) head [3] was proposed recently as a modification of the head described above to meet the requirements for practical use. As illustrated in Fig. 8.2, the head structure has a novel coil and a dual return yoke. The coil consists of a pair of windings in mutually opposite current directions, generating a cusped field. The main pole is placed in an off-center arrangement of the axisymmetric coil field to be energized strongly. The recession height of the outermost conductor of each winding is set at zero. For this coil configuration, it is easy to increase the number of coil turns so that the coil is useful at sufficiently low

K. Yamakawa (✉)
Akita Research Institute Of Advanced Technology (AIT), 4-21 Sanuki, Araya, Akita 010-1623, Japan
e-mail: yamakawa@rdc.pref.akita.jp

T. Osaka et al. (eds.), *Electrochemical Nanotechnologies,*
Nanostructure Science and Technology, DOI 10.1007/978-1-4419-1424-8_8,

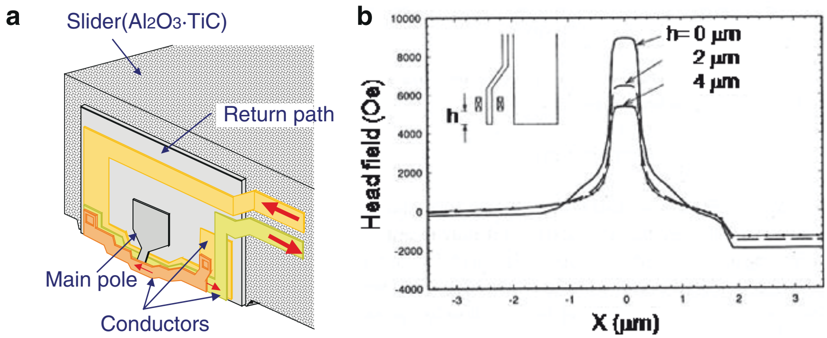

Fig. 8.1 (**a**) Schematic illustration of thin film head with a helical coil at the main pole tip. (**b**) Dependence of field distribution on coil recession height, *h* [2]. © 1999 IEEE

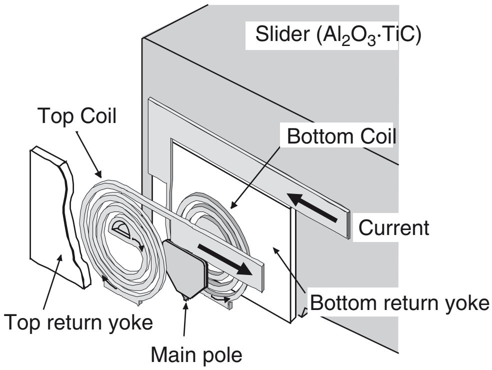

Fig. 8.2 Schematic illustration of CF-SPT head

current for practical use. The return yoke consists of two planar magnetic films. The main pole must be centered between these two films. This configuration has resolved the problem preventing its practical use; previously used conventional single pole heads having a one-side return yoke are vulnerable to stray fields. The CF-SPT head is anticipated for use in future high-density recording, although SPT heads modified from ring type heads for longitudinal recording have been used in first-generation commercial perpendicular recording systems.

In figures, use italic for variables.

8.2 Feasibility of Head Fabrication

The CF-SPT head has a simply stacked structure comprising planar films of magnetic, conductive and insulating materials, except for the connection part between the two coil windings. Therefore, the fabrication process of this head uses simpler techniques than those used for conventional heads. The CF-SPT head is fabricated using wet processes. The electrodeposition technique has been widely used for manufacturing conventional recording heads because it presents distinct advantages such as a high aspect ratio deposition, precise definition of pattern width, and a high deposition rate. To increase the track density, the critical dimension of the pole tip has been reduced by adopting advanced lithography techniques, reaching 40 nm, which corresponds to more than 500 Gbit/in^2 [4]. Electrodeposition will continue to be an important technology for manufacturing heads in the future also.

The head fabrication procedure involving wet processes is described below. As depicted in Fig. 8.3, a bottom-return yoke is first formed using electrodeposition. A soft magnetic material, e.g. CoNiFe, is electrodeposited on a sputter-deposited seed layer such as NiFe/Ti (Fig. 8.3a), which will be described later in detail together with the main pole fabrication. A SiO_2 insulating layer is then sputter-deposited on it. In the next step, a bottom coil is fabricated using a damascene process (Fig. 8.3b), which will also be described later in detail. After deposition of the insulating layer, the main pole material is electrodeposited on a sputter-deposited seed layer (Fig. 8.3c). Next, a Cu stud is made to connect the bottom and the top coils at their center and an insulating layer is deposited to planarize the surface. Then, a top coil is formed in the same manner as that of the bottom coil (Fig. 8.3d), which is followed by deposition of an insulating layer. At the final step, a top-return yoke is formed by electrodeposition (Fig. 8.3e), then, an insulating material as a protective layer is sputter-deposited. After completion of these wafer processes, the head wafer is cut into individual pieces and the ABS is formed by polishing (Fig. 8.3f).

In the test fabrication, the soft magnetic material of CoNiFe [5], with B_s of 2 T as developed by the Osaka group of Waseda University, was used for both the main pole and the return yoke. The CoNiFe film, with a target composition of $Co_{63}Ni_{13}Fe_{24}$, was electrodeposited using a paddle plating system, as depicted in Fig. 8.4, with the plating bath of the composition presented in Table 8.1. In addition, a frame plating method in a magnetic field to induce magnetic anisotropy was applied to form the main pole and the return yoke. The deposited film exhibited

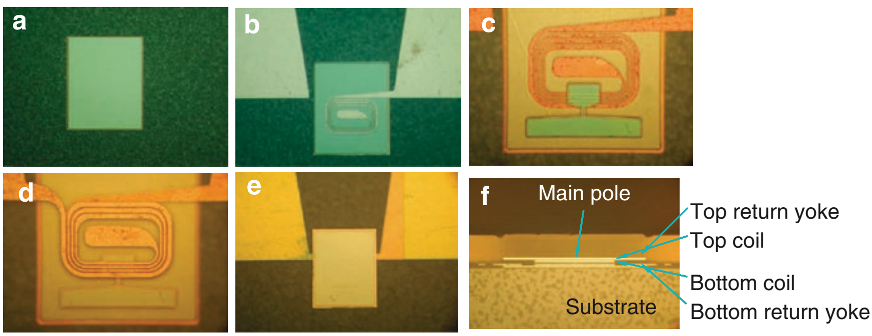

Fig. 8.3 Main process steps of CF-SPT head fabrication; (**a**) bottom return yoke, (**b**) bottom coil, (**c**) main pole, (**d**) top coil, (**e**) top return yoke, and (**f**) ABS

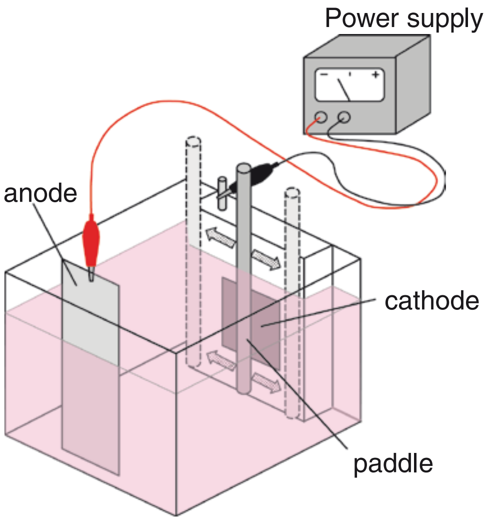

Fig. 8.4 Paddle plating system

Table 8.1 Plating bath composition for CoNiFe soft magnetic material

Chemicals	Concentration (mol/dm^3)
H_3BO_3	0.4
NH4Cl	0.28
$CoSO_4 \cdot 7H_2O$	0.064
$NiSO_4 \cdot 6H_2O$	0.2
$FeSO_4 \cdot 7H_2O$	0.011
SDS	10 ppm
pH	2.8
Current density	20 mA/cm^2
Agitation speed	144 cpm
Bath temperature	18–21°C
Counter electrode	Co plate
Magnetic field	100 Oe
Working electrode	Cu/Ti/glass (1 inch square)

uniaxial anisotropy, whose easy axis is aligned in the field direction, with low coercivity for widely varying film thicknesses, as depicted in Fig. 8.5.

The top and the bottom coils were fabricated using a damascene process. Coil trenches were formed in a SiO_{2}- insulating layer using reactive ion etching. A seed layer for electrodeposition such as a Cu/Ti stacked layer was sputter-deposited onto the etched surface. Then, the Cu electrically conductive material was electrodeposited on the seed layer using generic copper sulfate solution. Finally, lapping was performed

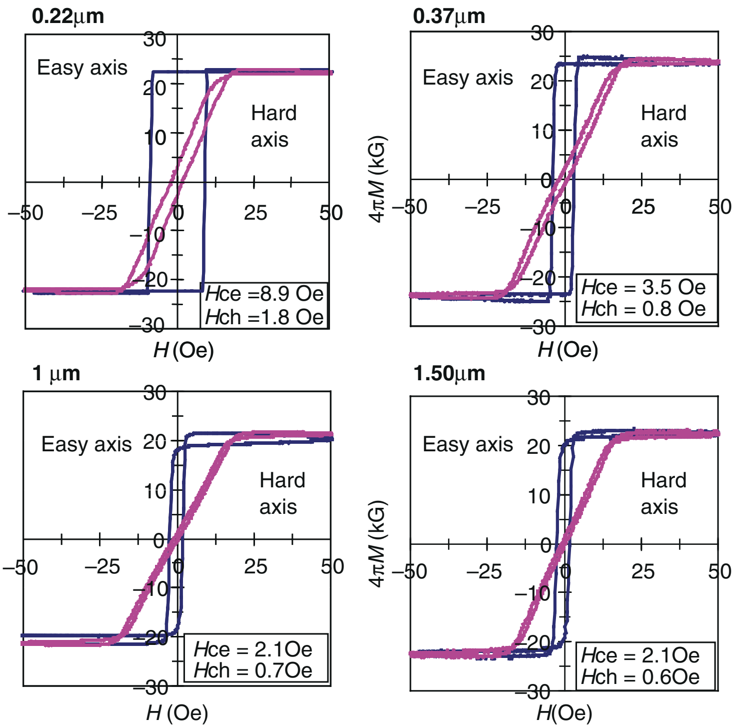

Fig. 8.5 Hysteresis loops of CoNiFe films in both easy and hard axes for various film thicknesses of 0.22–1.50 µm

to remove the excess Cu layer material. Coil pitch is an important parameter that influences the head efficiency because it governs the effective coil recession. The coil pitch is expected to be reduced. In very narrow pitches required for future high-density recording heads, forming the seed layer in the trenches with high aspect ratio will become problematic. For this issue, the new process technique developed for interconnects in ULSI [6] is useful for seed layer deposition. In the process, the NiB seed layer electroless-deposited on the self-assembled-monolayer (SAM) can be formed in high-aspect-trench patterns with excellent uniformity and conformability. Figure 8.6 shows the cross section of the Cu-filled trench pattern formed with the NiB/SAM seed layer. From this result, a narrow pitch of less than 1 µm is expected.

8.3 Performance of CF-SPT Head

In the CF-SPT head, the main pole is energized using a part of the cusped field generated by the opposing coil conductors. Field calculations using finite element method (FEM) revealed that the fields created at the main pole by the cusp coil and

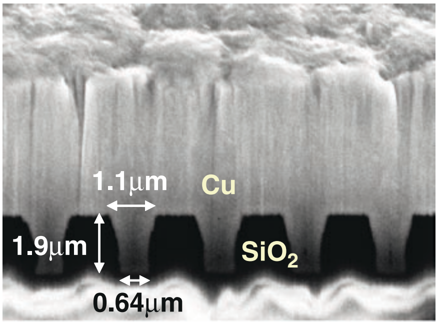

Fig. 8.6 Cu-filled coil trench using a NiB/SAM seed layer

the helical coil wrapped around the pole tip like that depicted in Fig. 8.2, are almost identical [7]. This similarity reflects that the cusp coil is equivalent in terms of main pole excitation to a helical coil with half the number of physical coil turns of the cusp coil. Therefore, the highest field applicable to the main pole tip located between the coil conductors and the field rapidly decreases with distance from the conductors [8]. This coil field scheme provides a stronger head field than that of the conventional SPT head with a recessed coil, as depicted in Fig. 8.7.

In addition to the head field strength, the coil field distribution confined between the opposing conductors uses a different pole-energizing method from the conventional head. The main pole tip region is magnetized preferentially. Therefore, only a small amount of flux generation is required, and it is localized at the main pole tip region. In contrast, for the conventional head, whole magnetic yokes are magnetized because of a closed magnetic circuit and a widely distributed coil field. Consequently, the CF-SPT head exhibits little field underneath the return yoke [7] that would affect the wide-area track erasure causing data loss by erasure of recorded information over a large area. In addition, the head inductance is small, helping to operate in the high data rate. An example of measured inductance as a function of frequency for the heads with effective two and three turn coils is depicted in Fig. 8.8 [9]. The resonance frequencies of the heads are much higher than that for the conventional ring-type head with seven turn coil, as shown in the figure. Therefore, superior performance of the CF-SPT head is expected.

Early SPT heads had a fatal flaw by which the head occasionally erased recorded signals without a writing operation when the head was exposed to an external stray field [10]. That phenomenon was a difficult issue for practical head implementation because the stray field easily magnetizes the main pole. For the head of a conventional yoke structure, the externally applied field, as depicted in Fig. 8.9, significantly degrades the signal output. In contrast, because the CF-SPT has a return yoke structure that sandwiches the main pole, the main pole can be shielded against a stray field. Consequently, the CF-SPT head has good stray field immunity, as depicted in Fig. 8.9.

As the head track width decreases, remanent magnetization of the main pole tip is likely to occur because of stress-induced anisotropy and increased shape anisotropy in the normal direction to the ABS. The field from this remanent magnetization can

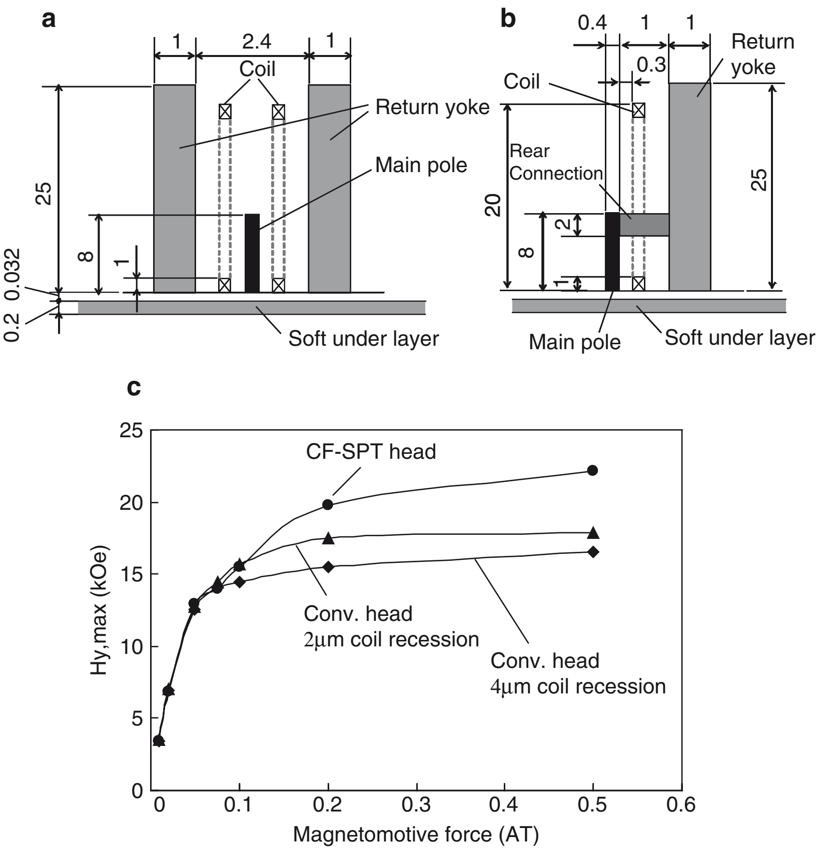

Fig. 8.7 Head model of (**a**) CF-SPT head and (**b**) conventional SPT head. (**c**) Comparison of head field for the CF-SPT head and conventional heads with various coil recessions

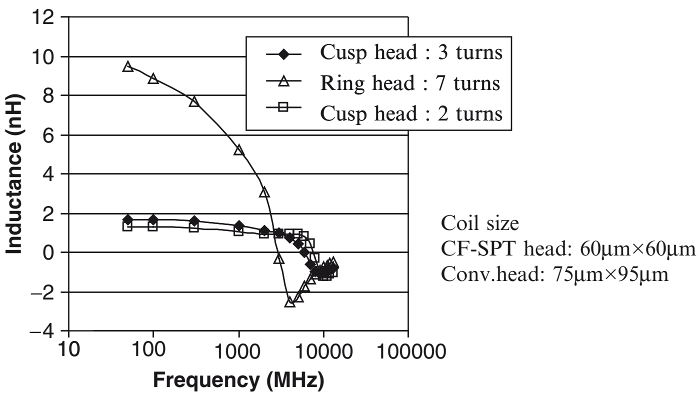

Fig. 8.8 Head inductance as a function of frequency for CF-SPT heads with various effective coil turns and a conventional head [9]. © 2003 IEEE

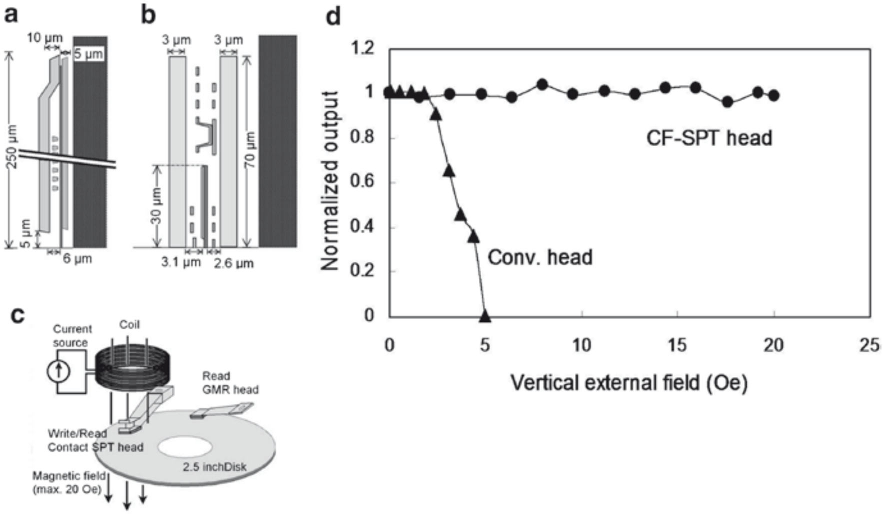

Fig. 8.9 Schematic illustration of (**a**) conventional SPT head and (**b**) CF-SPT head. (**c**) Experimental setup for stray field immunity. (**d**) Influence of the stray field on signal decay for CF-SPT head and conventional head

cause another type of head-induced erasure or pole erasure of recorded signals, even in an environment with no stray field [10]. The pole erasure can be eliminated through several means to align the magnetization in the track width direction. These solutions are a multilayer film structure [11], high anisotropy material [12], controlling stress-induced anisotropy [13], and the proper aspect ratio of the pole tip [14]. In addition, optimization of the main pole shape is a countermeasure for avoiding pole erasure. As depicted in Fig. 8.10, the main poles with different flare angles display different domain structures. The conventional flare angle of 45° exhibits an irregular domain structure containing a wall at the center running in the direction parallel to the flux propagation. In contrast, for 14°, a regular closed domain structure is realized by which the magnetization in the center domains lies in the track-width direction, as depicted in Fig. 8.10a. These domain structures show different signal decay over time. As depicted in Fig. 8.10b, the output signal decreases significantly for a 45° flare angle, although no signal deterioration is observed for the 14° flare angle. This difference suggests that the irregular domain structure causes the remanence of the pole tip. Consequently, domain control by optimizing the pole shape is an effective means to eliminate the pole erasure.

8.4 Advanced CF-SPT Head

Introduction of controlled inter-granular exchange coupling and hard/soft stacked layer design with inter-layer exchange coupling has been considered for granular media to alleviate writability problems for increased media anisotropy.

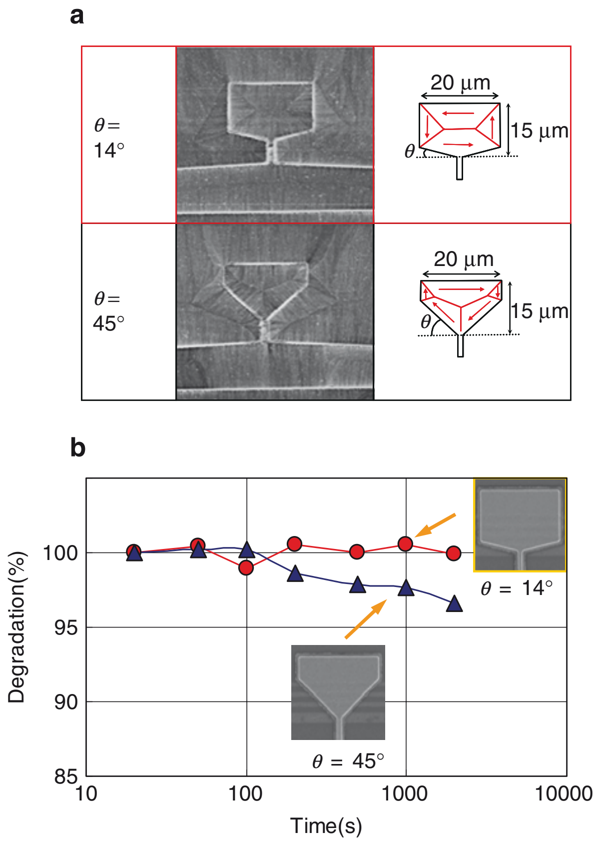

Fig. 8.10 (**a**) Effect of flare angle on domain structure of main pole. (**b**) Signal decay with time for different flare angles

Moreover, discrete track media, which enable the use of larger track-width writing heads, thereby providing a stronger head field than that for continuous media and bit-patterned media that have large switching volume, have been proposed as promising candidates for future high-density recording media. Nevertheless, a still larger head field will be necessary because the head track width will be continuously narrowed for an increased recording density. Furthermore, a higher field gradient is required because reduction of transition noise of granular media including discrete track media and an increased write-timing margin for bit-patterned media are responsible for the head field gradient and for the media property.

A shield structure has been proposed to improve the field gradient where the shield yoke is placed near the main pole [15, 16]. An example of a shielded SPT head based on a CF-SPT head [17] is depicted in Fig. 8.11a. The shield yoke absorbs the magnetic flux emanating from the side of the main-pole and prevents it from

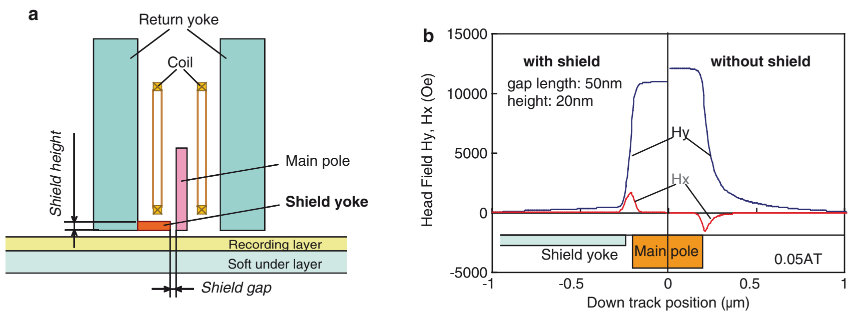

Fig. 8.11 (**a**) Structure of shielded CF-SPT head. (**b**) Comparison of head field between shielded and normal CF-SPT head

flowing into the medium. Consequently, the field gradient observed at the medium position is improved at the cost of the deterioration of recording flux, or head field strength, as depicted in Fig. 8.11b. Field strength loss occurs because the shield is small for an optimized shield design and the head exhibits no negative under-shoot observed for a shielded head modified from a conventional ring type head.

Shield design optimization for the CF-SPT head shows that critical dimensions such as shield gap length and shield height are expected to be in the order of a few tens of nanometers, as shown in Fig. 8.12. It is difficult to realize such a small shield structure using normal head fabrication techniques. However, the fabrication of a shielded CF-SPT head by a unique process has been demonstrated [17]. This process is as follows: a soft magnetic material is deposited on the head surface followed by focused ion bead (FIB) milling to form the shield gap, as depicted in Fig. 8.13. Improvement in writing resolution was actually obtained for the fabricated shield head.

On the analogy of a pole piece of an electromagnet, a main pole with a tapered structure is expected to produce a large field in association with the medium soft underlayer, thereby surpassing the material's limitation. The results of analytical calculations, depicted in Fig. 8.14, show that a tapered pole with a pyramidal shape generates a larger field for a larger base core size, W_2 and Tm_2, which engenders the possibility of a field beyond the saturation magnetization of the pole material [18–20]. In the figure, the stepped type of main pole is also shown to exhibit a large field, but the field is low compared to the tapered pole, especially for a large base core size. The reason for the strong fields of these heads, a so-called multi-surface pole head [19], is that the field from the charge appearing on the tapered surfaces is superimposed on the field from the charge on the pole tip surface. This mechanism suggests that the head field depends on the area of the tapered surface. Figure 8.15 compares the fields for the three different pole structures: tapered structures in both the down track and cross track directions, tapered structure only in the down track direction and no tapered structure [21]. The all-round tapered pole exhibits a much stronger field than the others. The tapered and the stepped pole

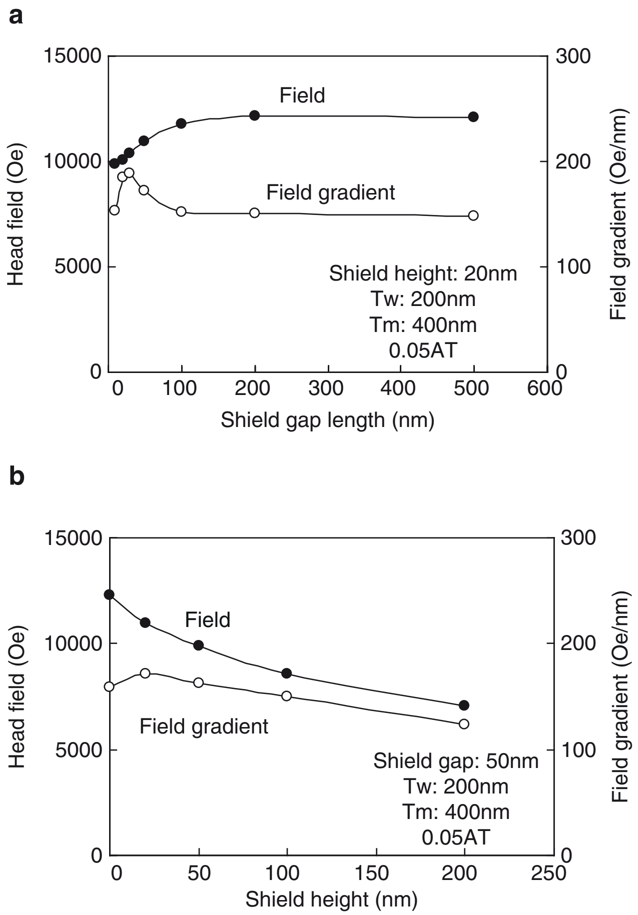

Fig. 8.12 Effect of (**a**) shield gap length and (**b**) shield height on head field strength and gradient

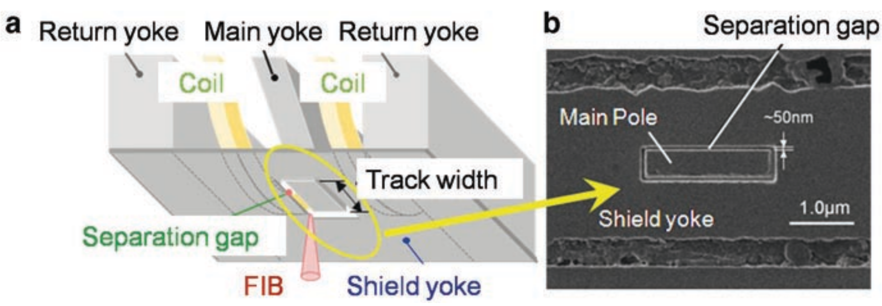

Fig. 8.13 (**a**) CF-SPT head with shield structure formed by FIB. (**b**) ABS view of shielded CF-SPT head

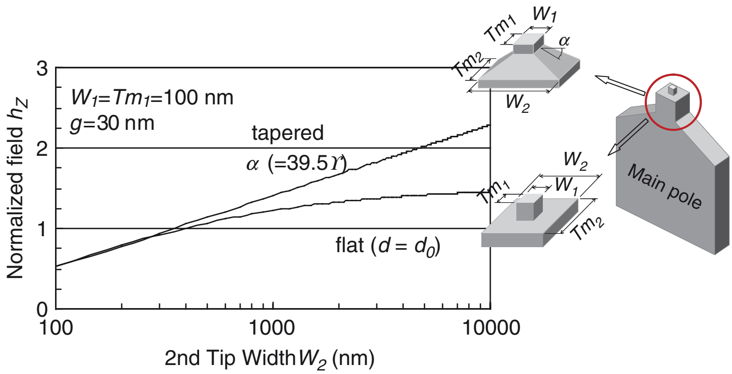

Fig. 8.14 Head field as a function of base core size, W_2 and Tm_2, for tapered and stepped main poles. Head field is normalized by saturation magnetization

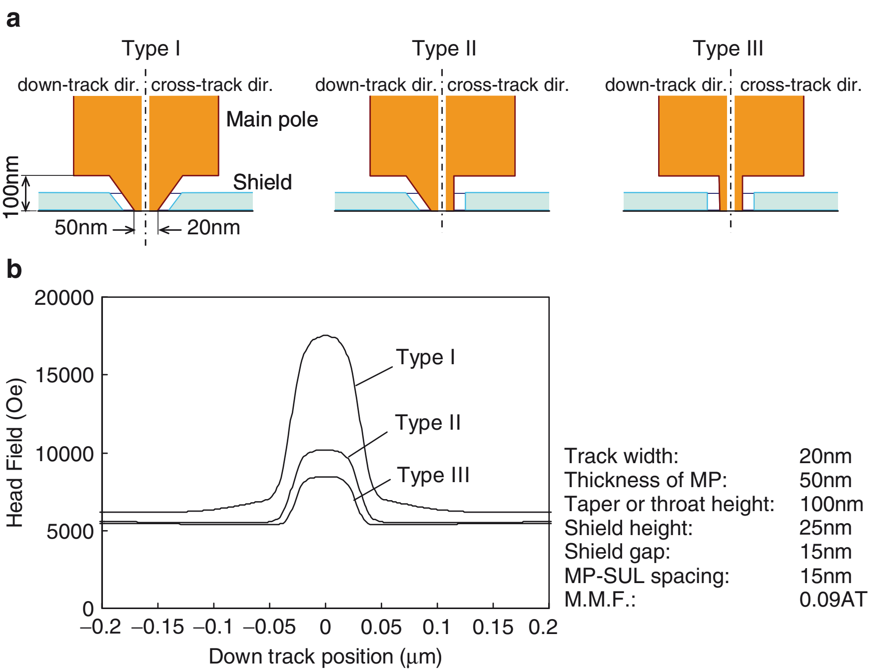

Fig. 8.15 (**a**) Variation of pole tip structure: *Type I* – tapered structure in both down and cross track directions; *Type II* – tapered only in the down track direction; *Type III* – no tapered structure. (**b**) Comparison of head fields for tapered main poles of various types

configurations fundamentally produce a large fringing field, especially at large magneto-motive forces, because of the field from the charge on the recessed surfaces. For that reason, the shield structure described previously must be combined with the main pole to obtain a sharp and strong field.

With a combination of the tapered pole structure and the shield structure, an advanced CF-SPT head has been proposed for 1 Tbit/in^2 recording [22]. As depicted in Fig. 8.16, the head has shields not only in the down track direction but also in the cross track direction to reduce the fringing field at adjacent tracks for achieving a high track density. The head exhibits high field strength and sharpness. Therefore, the CF-SPT head is a promising candidate as a writing head for future high-density recording. This advanced head is challenging in terms of its manufacture because of its structural complexity and nanoscale dimensions. It is expected to be a *breakthrough* development in resolving issues with the help of advanced nanoscale electro-deposition and electroless-deposition techniques.

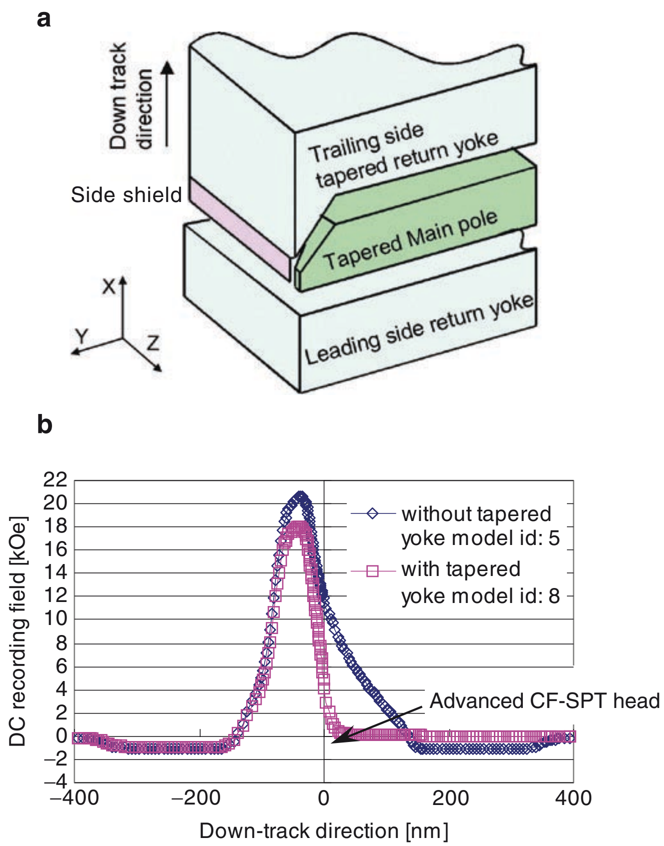

Fig. 8.16 Structure, cut at the track center (**a**), and field distribution (**b**) of an advanced CF-SPT head [22]. © 2003 IEEE

References

1. Iwasaki S, Nakamura Y (1978) The magnetic field distribution of a perpendicular recording head. IEEE Trans Magn 14:436–438
2. Muraoka H et al (1999) Low inductance and high efficiency single-pole writing head for perpendicular double layer recording media. IEEE Trans Magn 35:643–648
3. Ise K et al (2000) High writing-sensitivity single-pole head with cusp-field coils. IEEE Trans Magn 36:2520–2523
4. Brankovic SR et al (2006) Pulse Electrodeposition of 2.4 T $Co_{37}Fe_{63}$ alloys at nanoscale for magnetic recording application. IEEE Trans Magn 42:132–139
5. Osaka T et al (1998) A soft magnetic CoNiFe film with high saturation magnetic flux density and low coercivity. Nature 392:796–798
6. Yoshino M et al (2005) All-wet fabrication process for ULSI interconnects technologies. Electrochim Acta 51:916–920
7. Yamakawa K et al (2002) A new single-pole head structure for high writability. IEEE Trans Magn 38:163–168
8. Yamakawa K et al (2007) FEM model analysis of single-pole-type heads with different coil structures. IEICE Trans Electron E90-C:1555–1560
9. George P et al (2003) High-frequency inductance measurements and performance projections made for cusp-field single-pole heads. IEEE Trans Magn 39:1949–1954
10. Payne W, Cain A, Bauldwinson M, Hempstead R (1996) Challenges in the practical implementation of perpendicular magnetic recording. IEEE Trans Magn 32:97–102
11. Nakamoto K et al (2004) Single-pole/TMR heads for 140-Gb/in^2 perpendicular recording. IEEE Trans Magn 40:290–294
12. Hirata K et al (2005) Material properties and domain structure influence on pole erasure occurrence in perpendicular recording heads. IEEE Trans Magn 41:2902–2904
13. Hirata K, Roppongi T, Noguchi K (2005) A study of pole material properties for pole erasure suppression in perpendicular recording heads. J Magn Man Mater 287:352–356
14. Gao KZ, Bertram HN (2002) 3-D micromagnetic simulation of write field rise time in perpendicular recording. IEEE Trans Magn 38:2063–2065
15. Mallary ML (1987) Vertical magnetic recording arrangement. US Patent #4 656 546
16. Mallary ML, Das SC (1992) Reissued #33 949
17. Ise K, Yamakawa K, Honda N (2003) High-field gradient cusp field single-pole writing head with front return yoke. IEEE Trans Magn 39:2374–2376
18. Takahashi S, Yamakawa K, Ouchi K (2001) 2 steps type of single pole head for ultra narrow track. Tech Rep IEICE MR2001-1:1-8
19. Takahashi S, Yamakawa K, Ouchi K (2002) Single-pole type head with multicharged surfaces for ultrahigh density recording. J Appl Phys 91:6839–6841
20. Gao KZ, Bertram HN (2002) Write field analysis and write pole design in perpendicular recording. IEEE Trans Magn 38:3521–3527
21. Ise K et al (2006) New shielded single-pole head with planar structure. IEEE Trans Magn 42:2422–2424
22. Kanai Y et al (2003) Recording field analysis of narrow-track SPT head with side shields, tapered main pole, and tapered return path for 1 Tb/in^2. IEEE Trans Magn 39:1955–1960